

Silica Hollow Spheres by Templating of Catanionic Vesicles

Hans-Peter Hentze, Srinivasa R. Raghavan,[†] Craig A. McKelvey,[‡] and Eric W. Kaler*

Center for Molecular Engineering and Thermodynamics, Department of Chemical Engineering, University of Delaware, Newark, Delaware 19716

Received August 16, 2002. In Final Form: December 4, 2002

A simple and effective means for obtaining hollow silica particles of controlled diameter from about 60 to 120 nm is presented. The synthesis utilizes equilibrium vesicles as templates for the directed growth of silica. Two different surfactant systems are used to form the vesicular templates: (a) mixtures of cetyltrimethylammonium bromide (CTAB) and sodium perfluorooctanoate (FC₇) and (b) mixtures of cetyltrimethylammonium tosylate (CTAT) and sodium dodecylbenzenesulfonate (SDBS). These templates were chosen because these mixtures of surfactants in water form unilamellar vesicles spontaneously that appear stable in the chemical environment required for silica synthesis. Tetramethoxysilane (TMOS) is added to the vesicular templates as a precursor for silica formation via acid-catalyzed hydrolysis and polycondensation. The morphology of the silica products as observed with transmission electron microscopy (TEM), quasi-elastic light scattering (QLS), and small-angle neutron scattering (SANS) is consistent with silica deposition at the vesicle surface, creating hollow silica particles with a 1–2-nm-thick shell and with a core diameter identical to that of the template. TEM reveals under different conditions either discrete hollow particles or networks of linked or aggregated hollow silica shells.

I. Introduction

The synthesis of materials structured on a nanometer scale is an intense and rapidly developing field of research. Nanostructured materials are potentially useful in a variety of applications such as catalysis, separations, and drug delivery. An effective and simple approach to preparing nanostructured materials involves template synthesis.^{1–3} Here, a usually nanostructured template directs the reaction of precursors toward the final product. A variety of different templating mechanisms have been described. In a transcriptive templating process, the reactants form products at the template interface, creating a cast of the template morphology. The template and the precursor may also cooperatively determine product structure in a synergistic templating process. Finally, controlled demixing of template and product can also lead to well-organized, complex morphologies in a so-called reconstructive morphosynthesis.

Hollow, spherical nanoparticles represent a class of materials that can be synthesized by template syntheses. Potential applications for such particles are in encapsulation, drug release, controlled drug delivery, or the manufacture of “nanofoams”. Hollow particles have been prepared from many templates, such as polyelectrolyte nanoparticles⁴, emulsion droplets,⁵ lyotropic phases exhibiting a multilamellar vesicular structure,⁶ or vesicular solutions.^{7,9}

So far, only multilamellar⁷ and kinetically stabilized unilamellar vesicles^{8–10} have been used as templates for silica synthesis. Pinnavaia et al. reported the template synthesis of multilamellar silica hollow spheres within vesicular solutions of gemini surfactants and their functionalization by incorporation of catalytic metal ion centers.⁷ Silica templating within mesophases of ionic block copolymers yields mesoporous morphologies that include vesicular structure elements,⁶ while kinetically stabilized unilamellar vesicles produced under shear have been used to create hollow silica particles.⁸ In the later case, TEM images suggest a transcriptive silica deposition mechanism; however, a flattening of the vesicles also occurs that was attributed to alcohol formation during the synthesis.

The success of templating schemes depends particularly on the stability of the template. In addition to being inherently stable, equilibrium vesicles are both simple and inexpensive to prepare. In contrast to most vesicular systems which form only when shear or other mechanical energy is applied, equilibrium vesicles form spontaneously in solutions of certain cationic and anionic surfactants.¹¹ The vesicles are unilamellar and attain an equilibrium size for a given surfactant ratio and concentration.¹² No change in equilibrium size and unilamellar morphology is observed on the time scale of years and the size is recovered after shear. Hollow organic polymer particles can be synthesized from an equilibrium vesicle template

* Address correspondence to this author.

[†] Current addresses: University of Maryland, Department of Chemical Engineering, College Park, MD 20742-2111.

[‡] Current addresses: Merck Research Laboratories, WP 78-304, Sumneytown Pike, West Point, PA 19486.

(1) Mann, S.; Burkett, S. L.; Davis, S. A.; Fowler, C. E.; Mendelson, N. H.; Sims, S. D.; Walsh, D.; Whilton, N. T. *Chem. Mater.* **1997**, *9*, 2300.

(2) Göltner, C. G.; Antonietti, M. *Adv. Mater.* **1997**, *9*, 431.

(3) Hoss, R.; Vögtle, S. *Angew. Chem., Int. Ed. Engl.* **1994**, *33*, 375.

(4) Caruso, F. *Chem. Eur. J.* **2000**, *6*, 413.

(5) Schacht, S.; Huo, Q.; Voigt-Martin, I. G.; Stucky, G. D.; Schüth, F. *Science* **1996**, *273*, 768.

(6) Krämer, E.; Förster, S.; Göltner, C. G.; Antonietti, M. *Langmuir* **1998**, *14*, 2027.

(7) Kim, S. S.; Zhang, W. Z.; Pinnavaia, T. J. *Science* **1998**, *282*, 1302.

(8) Hubert, D. H. W.; Jung, M.; Frederik, P. M.; Bomans, P. H. H.; Meuldijk, J.; German, A. L. *Adv. Mater.* **2000**, *12*, 1286.

(9) Hubert, D. H. W.; Jung, M.; German, A. L. *Adv. Mater.* **2000**, *12*, 1291.

(10) Hubert, D. H. W. Ph.D. Thesis, Technische Universiteit Eindhoven 1999; 120–132.

(11) Kaler, E. W.; Murthy, A. K.; Rodriguez, B. E.; Zasadzinski, J. A. N. *Science* **1989**, *245*, 1371.

(12) Jung, H. T.; Coldren, B.; Zasadzinski, J. A.; Iampietro, D.; Kaler, E. W. *Proc. Natl. Acad. Sci. U.S.A.* **2001**, *98*, 1353.

formed by cationic and anionic surfactant mixtures.^{13,14} The polymer particles were formed by the cross-linking of an unsaturated monomer (such as divinyl benzene) present in the vesicle bilayer. The initial vesicle size is reproduced in the final polymer product and the hollow particles could be completely dried and resuspended in water without any loss of structure.

Here, we enlarge the scope of our templating approach to inorganic (silica) nanoparticles. Such particles are potentially suited for use as catalysts, hosts for chemical reactions, coatings, and many other applications.¹⁵ Two different thermodynamically stabilized vesicle templates of cationic and anionic surfactants are investigated in this study: (a) cetyltrimethylammonium bromide (CTAB) and sodium perfluorooctanoate (FC₇)¹⁶ and (b) cetyltrimethylammonium tosylate (CTAT) and sodium dodecylbenzenesulfonate (SDBS).¹⁷ In such catanionic mixtures, strong electrostatic interactions between the oppositely charged headgroups initiate bilayer formation. Additionally, the combination of hydrocarbon and fluorocarbon chains in the vesicle bilayer of the CTAB/FC₇ system leads to a high elastic constant for the bilayer; in turn, this leads to remarkably monodisperse vesicles.¹² The vesicle bilayer in the CTAT/SDBS system consists only of hydrocarbon chains and are thus more flexible than in the CTAB/FC₇ template.

The vesicular templates used for this study are capable of directing silica growth. Hollow silica nanoparticles are formed in each case by deposition of silica on the vesicles. These particles are characterized by quasi-elastic light scattering (QLS), small-angle X-ray scattering (SAXS), small-angle neutron scattering (SANS), and transmission electron microscopy (TEM). Variations in silica morphology with the type and composition of the template are discussed to illustrate the scope and limitations of this approach.

II. Experimental Section

II.1 Preparation of Equilibrium Vesicles. The surfactants cetyltrimethylammonium bromide (CTAB, Aldrich), cetyltrimethylammonium tosylate (CTAT, Aldrich), sodium dodecylbenzenesulfonate (SDBS, TCI America), and sodium perfluorooctanoate (FC₇, Lancaster) were used as supplied. Vesicular solutions were prepared from surfactant stock solutions in 0.001 M hydrochloric acid. Samples obtained by mixing appropriate amounts of the stock solutions were stirred in a 100-mL round-bottom flask at room temperature for 14 days to achieve equilibrium size, as monitored by dynamic light scattering. The composition of the catanionic surfactant solution is given by the parameters γ and δ , where γ is the total surfactant concentration and δ is the cationic fraction of the total surfactant. For SANS measurements, water was replaced by equimolar amounts of D₂O (Cambridge Isotope Laboratories).

II.2 Silica Synthesis. The precursor, tetramethoxysilane (TMOS, Aldrich), was added to 10 mL of the vesicular template. The weight ratio of TMOS to surfactant was varied between 0.5 and 2. After addition of the precursor, the solution was stirred for 15 min to achieve a transparent, single-phase solution. For light scattering studies, about 1 mL of the reaction mixture was

transferred into an ampule that was then flame sealed. The samples were kept at room temperature without stirring.

II.3 Methods and Instruments. Quasi-elastic light scattering (QLS) measurements were performed using a Brookhaven BI200SM goniometer, a BI9000-AT correlator, and a Lexel 300 mW Ar laser ($\lambda = 488$ nm). The scattering angle was 90° for all measurements. The hydrodynamic diameter was obtained from the Stokes–Einstein relationship and the diffusion coefficient as measured by the method of cumulants.¹⁸

Small-angle neutron scattering (SANS) experiments were made at the NG-3 spectrometer at the National Institute of Standards and Technology (NIST) in Gaithersburg, MD. Measurements were performed at detector distances of 13, 4.5, and 1.3 m, corresponding to a scattering vector range of 0.05–5 nm⁻¹. The wavelength of the neutrons used was 6 Å with a spread of 15%. Data analysis and scattered intensity corrections for background scattering and detector sensitivity were done using standards provided by NIST.

Transmission electron microscopy (TEM) was used to probe the structure of the silica particles. TEM samples were prepared directly from solution or after purification by centrifugation and washing with water and methanol. Carbon-coated grids were used as supports for the solvent casted samples, which were examined using a Zeiss EM 912 OMEGA electron microscope.

II.4 SANS Modeling. A core–shell model was used to fit the SANS spectra for both the vesicles in the template and the templated hollow silica particles. The adjustable parameters for this model are the template core diameter, template shell thickness, silica shell thickness, and polydispersity. These parameters were simultaneously varied to minimize the value of χ^2 for the model fit to each SANS spectrum (with and without silica). In the templated particles, the actual volume fraction of scatterers is calculated from a mass balance assuming that all the TMOS forms silica. It is further assumed that the silica deposits on both sides (inner and outer) of the vesicle bilayer. The silica core diameter can then be calculated from the diameter of the vesicle core and the silica shell thickness.

The scattering length densities for each component were calculated by summing the scattering amplitudes of each group or atom in a molecule and dividing this total by the sum of the respective volumes. For CTAB, FC₇, and silica, the calculated scattering length densities were $-1.5 \cdot 10^{-7} \text{ Å}^{-2}$, $3.7 \cdot 10^{-6} \text{ Å}^{-2}$, and $3.7 \cdot 10^{-6} \text{ Å}^{-2}$, respectively. The scattering length density of D₂O is $6.3 \cdot 10^{-6} \text{ Å}^{-2}$.

III. Results and Discussion

A sol–gel process involving the TMOS precursor was used to synthesize silica in solution. The hydrolysis of TMOS occurs readily under acidic conditions, and a pH of 3 was therefore chosen. The phase behavior and microstructure of CTAB/FC₇ and CTAT/SDBS solutions are well documented for neutral pH,¹⁷ and the relevant portions of the phase diagram are replotted in Figure 1. Compositions within the unilamellar vesicle lobes were chosen for the templates. The phase behavior at pH 3 has not been studied in detail, but visual observations of the solutions at pH 3 show characteristics similar to those at neutral pH, namely, a bluish tinge indicative of light scattering from vesicles.

Quasi-elastic light scattering (QLS) was used to measure the CTAB/FC₇ vesicle size in the acidic solutions (Figure 2). Vesicles reach their equilibrium size in about 14 days. The equilibrium size of the vesicles for a composition of $\delta = 0.85$ and $\gamma = 3$ wt % is 67 nm. At a slightly different concentration ($\delta = 0.85$ and $\gamma = 2$ wt %), the equilibrium aggregate size is 53 nm. The latter composition at neutral pH had an equilibrium hydrodynamic diameter of 64 nm.

Small-angle neutron scattering (SANS) was used to further study the CTAB/FC₇ vesicles formed in acidic solution (in D₂O). The SANS spectrum for a sample with a composition of $\delta = 0.80$ and $\gamma = 1.67\%$ is shown in Figure

(13) Morgan, J. D.; Johnson, C. A.; Kaler, E. W. *Langmuir* **1997**, *13*, 6447.

(14) McKelvey, C. A.; Kaler, E. W.; Zasadzinski, J. A.; Coldren, B.; Jung, H. T. *Langmuir* **2000**, *16*, 8285.

(15) *Hollow and Solid Spheres and Microspheres: Science and Technology Associated With Their Fabrication and Application*; Wilcox, D. L., Berg, M., Bernat, T., Kellermann, D., Cochran, J. K., Eds.; Materials and Research Society Proceedings: Pittsburgh, PA, 1995; Vol. 372.

(16) Iampietro, D. Ph.D. Thesis, University of Delaware, 1999; 124.

(17) Kaler, E. W.; Herrington, K. L.; Murthy, A. K.; Zasadzinski, J. A. N. *J. Phys. Chem.* **1992**, *96*, 6698.

(18) Koppel, D. E. *J. Chem. Phys.* **1972**, *57*, 4818.

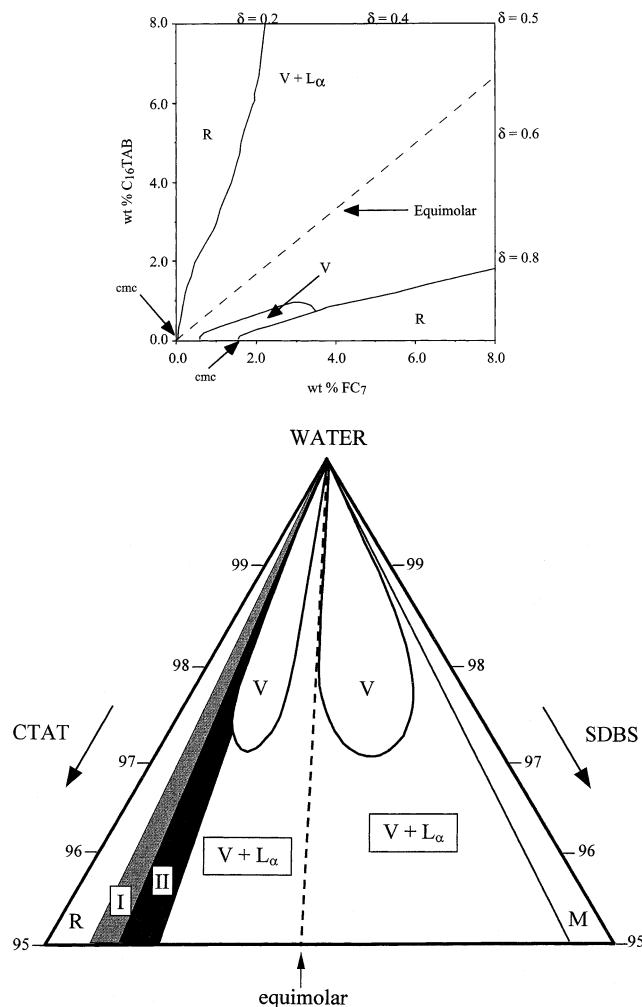


Figure 1. Phase diagrams for (a) CTAB/FC₇/water and (b) CTAT/SDBS/water at neutral pH and 25 °C.

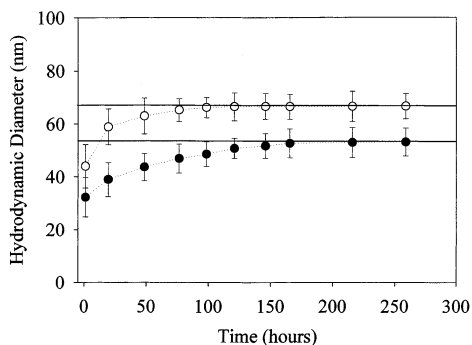


Figure 2. Hydrodynamic diameter of CTAB/FC₇ vesicle templates during equilibration at pH 3. The closed circles are for vesicles at $\gamma = 1.9$, $\delta = 0.8$. The open circles are for vesicles at $\gamma = 3.5$, $\delta = 0.85$.

3. The spectrum displays a q^{-2} dependence of the scattered intensity, which is a signature of scattering from bilayers and membranes.¹⁹ The spectra are thus qualitatively consistent with the presence of vesicles in solution. Fitting the spectra to the core-shell model yields a core diameter of 41.4 nm, a shell (bilayer) thickness of 2.2 nm, and a polydispersity of 0.25. These are in good agreement with the previously published results of 42.0 nm, 2.8 nm, and 0.22, respectively, for a CTAB/FC₇ sample of similar composition but without added acid.¹⁶

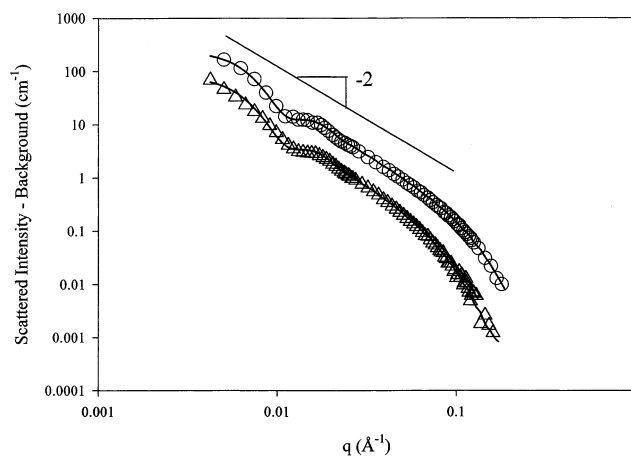


Figure 3. SANS data, I -Background vs q , for the CTAB/FC₇ template and template with silica in D₂O. The template (open circles) composition is $\gamma = 1.67\%$ and $\delta = 0.80$ with a pH adjusted to 3 by addition of concentrated HCl. The sample with silica (triangles) is $\gamma = 0.238$ wt % and $\delta = 0.80$ with 0.238 wt % TMOS added (corresponding to a TMOS to surfactant mass ratio of 1). A core-shell model including an excluded volume interaction with four adjustable parameters was used to fit both spectra simultaneously (solid lines). The template core diameter (41.4 nm), template shell thickness (2.2 nm), silica shell thickness (3.3 nm), and polydispersity (24.5%) were obtained by minimizing χ^2 for the two spectra.

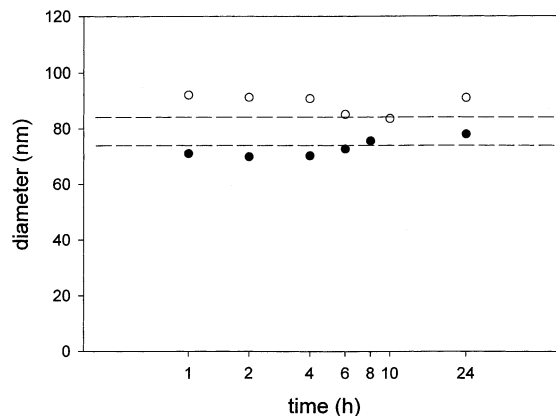


Figure 4. Hydrodynamic diameter during silica formation in CTAB/FC₇ systems at pH 3. The closed circles are for vesicles at $\gamma = 1.9$, $\delta = 0.8$, and a TMOS:surfactant ratio of 1. The open circles are for vesicles at $\gamma = 3.5$, $\delta = 0.85$, and a TMOS:surfactant ratio of 1.

Following the fourteen day equilibration period, TMOS was added to each vesicular solution at a weight ratio 1:1 with respect to the total surfactant concentration. The solution immediately became slightly turbid on addition of the hydrophobic precursor. After stirring for 15 min, a transparent solution again emerged, and this was kept without further agitation at room temperature to complete the reaction. As the sol-gel reaction proceeds, there is an increase in the intensity of light scattered from the sample, as observed during QLS experiments (as a result of an increasing optical density by silica formation). However, only small changes in hydrodynamic diameter are observed during the course of the reaction (Figure 4).

Triton X-100, a nonionic surfactant that can micellize vesicles and destroy membranes, was added to the solutions as a qualitative test for changes due to reaction. In all cases, the vesicular template is easily destroyed at low concentrations (<1 g/l) of Triton X-100 whereas the templated silica particles remain in stable dispersion. Addition of Triton X-100 to the templated silica causes a

(19) Porod, G. In *Small-Angle X-Ray Scattering*; Kratky, O., Glatter, O., Eds.; Academic Press Inc.: London, 1982; p 17.

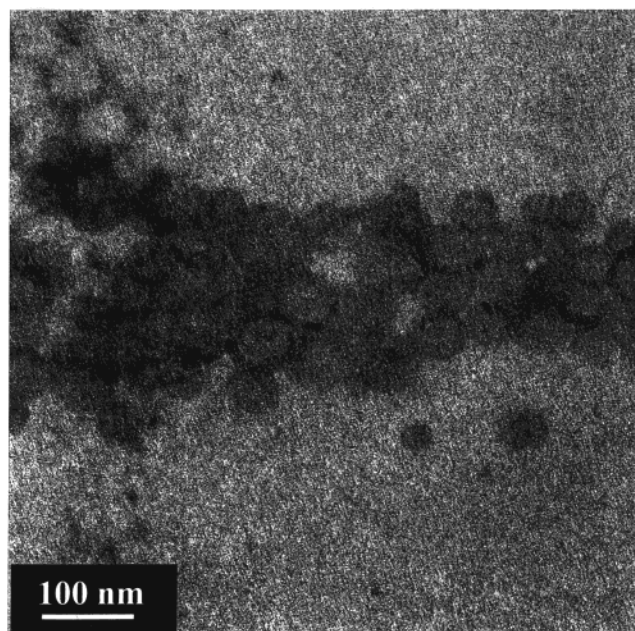


Figure 5. TEM micrograph of untreated silica sample SVT 2 templated from CTAB/FC₇ at a composition of $\gamma = 1.9$, $\delta = 0.8$, and a TMOS:surfactant ratio of 1.

small increase in the hydrodynamic diameter, as measured by QLS, which is consistent with the adsorption of Triton X-100 onto the surface of the hollow silica particles.

TEM images confirm the formation of hollow silica particles in the final product (Figure 5 and Table 1). Here, a drop of reacted solution was applied on the TEM grid without any further purification or staining. Following drying, hollow particles of templated silica are visible. Because of the formation of an unstructured surfactant film during drying, the observed contours are not sharp. The particles also appear to aggregate during the drying process. It is evident from the images that the silica is deposited on the surfactant bilayers. Attempts were also made to isolate the silica free of surfactant by repeated washing with methanol followed by centrifugation (Figure 6). Although most of the hollow structures collapsed or fused because of the centrifugal forces, TEM did reveal the existence of single hollow particles, an example of which is also shown in the CTAT/SDBS templated silica (Figure 7). Silica deposition on the vesicle is particularly evident in this image and the nonuniform shell thickness is similar to that observed by Hubert et al.⁹

SANS was also used to characterize the vesicle-templated silica particles in dispersion in D₂O (Figure 3). The composition of the vesicle template was $\gamma = 1.67\%$ and $\delta = 0.80$ at pH 3. To this solution, 1.67% TMOS was then added, corresponding to 1:1 (TMOS: surfactant) by weight. After the silica synthesis, the product was diluted with D₂O by a factor of 4. The scattering from this product also shows a q^{-2} dependence and is qualitatively similar to that of the original template. This suggests that hollow particles with thin shells exist, that is, the vesicular structure is preserved. The concentration of scatterers in the templated product is lower because of the dilution, which is why the scattered intensity is lower. Fitting the SANS spectra from the hollow silica product to the core-shell model gives an overall shell thickness of 3.3 nm, which includes both silica layers and the surfactant bilayer. In turn, this suggests that about 1.1 nm of the shell is due to the silica network.

Templated silica dispersions prepared with a TMOS to surfactant weight ratio of 1:1 were stable for several weeks.

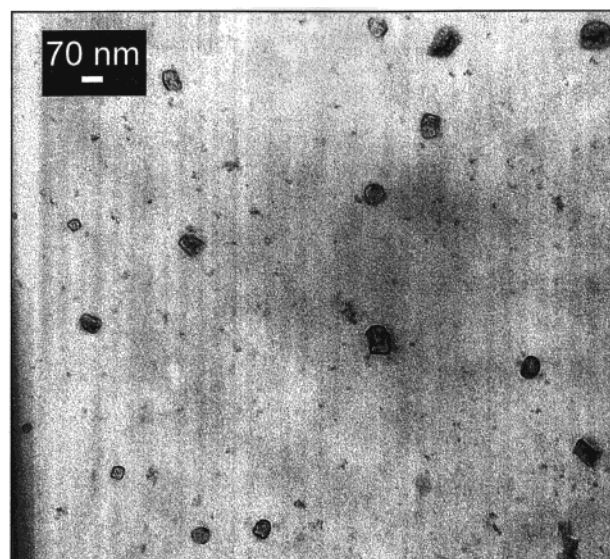


Figure 6. TEM micrograph of silica sample SVT 5 templated from CTAB/FC₇ at a composition of $\gamma = 3$, $\delta = 0.85$, and a TMOS:surfactant ratio of 1. Before preparation for TEM, the sample was purified by centrifugation and washing with methanol.

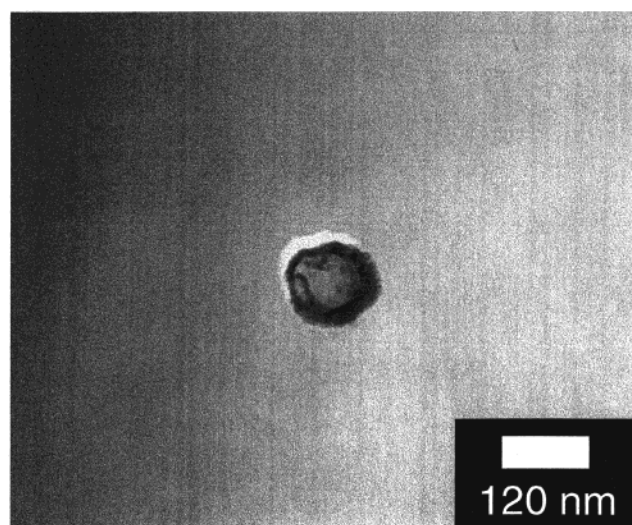


Figure 7. TEM micrograph of a silica vesicle washed with methanol and templated from CTAT/SDBS at a composition of $\gamma = 1$, $\delta = 0.7$, and a TMOS:surfactant ratio of 1.

For higher TMOS concentrations, solid silica particles are formed in the aqueous phase in addition to silica hollow spheres. In these cases, the particles appear to aggregate into branched networks causing a macroscopic gelation of the sample. Some aggregation was always observed in the CTAT/SDBS system over long periods of time. The hydrodynamic diameter of these samples remains unchanged for the first 12 h of the reaction, but eventually the dispersions phase separate and a strong increase in size is observed (QLS results not shown). During the initial part of the reaction (after 2 h), silica can be isolated by washing the solution with methanol to remove the surfactant followed by centrifugation. The longer term aggregation may be due to several reasons. First, methanol is generated during the reaction and this could affect the stability of the vesicle bilayers, thereby causing a loss of the tightly bound silica structure. Also, the silica surface charge is a function of pH, which drops as the reaction proceeds, thus influencing colloidal stability. Finally, with excess hydrophobic TMOS, the bilayer could swell ap-

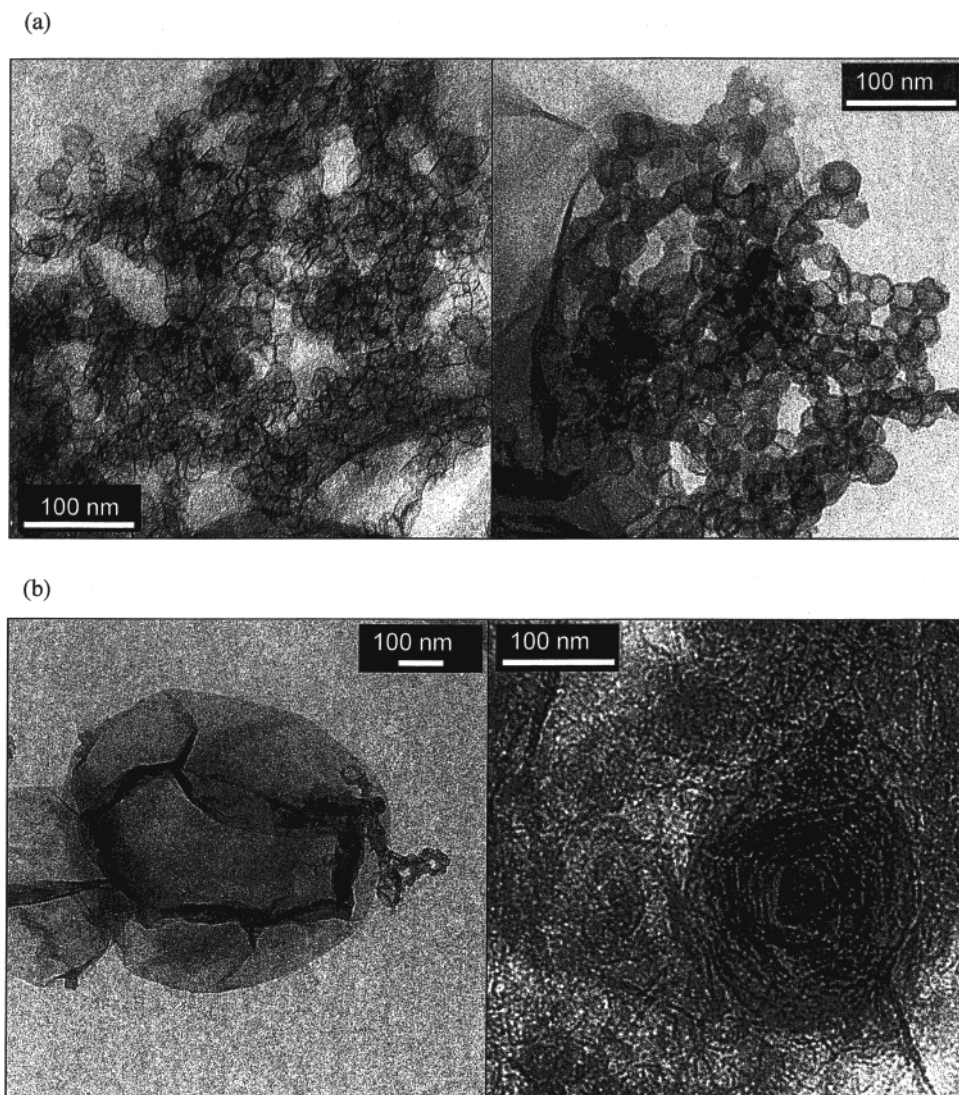


Figure 8. TEM micrographs of silica templated in the biphasic L_{α} /vesicle phase of CTAB/FC₇/water ($\delta = 0.44$ and $\gamma = 2$ wt %). (a) Silica isolated after 24 h: only small vesicular and layerlike structures are observed. (b) Silica isolated after 48 h: multilamellar and giant vesicular structures are observed.

precipitously causing microstructure perturbations or even a shift toward a flat lamellar architecture. Similar phase separation and gelation of the silica product were reported by Hubert⁹ et al. in vesicle templating studies for samples with high TMOS:surfactant ratios, and those authors suggest that the lowering of the pH was the prime driver for the observed silica aggregation.

Template synthesis is not only a powerful means for materials synthesis, but it can also contribute to the determination and analysis of self-organized morphologies. For instance, cubic, lamellar, hexagonal, and transition morphologies of mesophases have been directly visualized by TEM after synergistic templating of lyotropic amphiphilic block copolymer mesophases.²⁰ The retention of structure was confirmed by polarized light microscopy, SAXS, and SANS,²¹ and in these cases comparisons of silica templated in the non-cross-linked mesophase with that of the cross-linked system revealed that no changes in morphology occurred during silica synthesis.²⁰ Thus, by direct imaging of the templated material it is possible to gain structural information that is difficult to obtain

from characterization of lyotropic mesophases by other techniques (e.g., cryo-TEM or freeze-fracturing). True one-to-one templating by sol-gel processes with retention of the parental order has also been observed for several other systems.²

In addition to silica morphologies templated in equilibrated vesicular phases, silicate reactions were also carried out in the biphasic lamellar/vesicular region of the CTAB/FC₇ phase diagram ($\delta = 0.44$; $\gamma = 2$ wt %, Figure 1) during equilibration. This is possible because the equilibration times of cationic surfactant systems can range from days to weeks, so that the templating reactions are rapid compared to the time to reach equilibrium. Immediately after mixing the surfactant solutions, the sample appears transparent and has a low viscosity. Within 1 day the solution becomes more viscous and opaque and exhibits a Maltese-cross texture when observed with a polarized light microscope. To examine the different silica morphologies formed during this equilibration process, TMOS was added to the freshly prepared solution of surfactants. After both 12 and 24 h, samples were drawn and the silica isolated by centrifugation and subsequent washing with methanol. Transmission electron micrographs show different morphologies in both silica fractions, namely, small hollow spheres, layerlike structures, and multilamellar

(20) Hentze, H.-P.; Krämer, E.; Berton, B.; Förster, S.; Antonietti, M.; Dreja, M. *Macromolecules* **1999**, *32*, 5803.

(21) Förster, S.; Berton, B.; Hentze, H.-P.; Krämer, E.; Antonietti, M.; Lindner, P. *Macromolecules* **2001**, *34*, 4610.

morphologies (Figure 8). Whereas the silica isolated after 12 h shows only small hollow spheres and some sheetlike structures (Figure 8a), the sample isolated after 24 h also contains replicas of giant vesicles and multilamellar structures in addition to smaller hollow spheres (Figure 8b).

Of course, these results alone may not shed light on how the lamellar phase forms because changes in morphology induced by the templating process cannot be excluded. Nonetheless, these results do hint at a sensible morphological evolution of the lamellar phase starting from small unilamellar vesicles and progressing to giant and multilamellar vesicular structures. The latter can be seen as an intermediate state between discrete vesicles and L_α -mesophases.

IV. Conclusion and Outlook

Silica hollow particles were synthesized in equilibrium vesicle solutions by sol-gel synthesis. Templating cat-anionic vesicles formed by CTAB and FC₇ leads to a 1:1 casting of the vesicle structure by the formed silica matrix. The silica hollow spheres formed are typically stable for weeks. Unishell silica hollow spheres were observed by TEM and also characterized by QLS and SANS. Similar results were observed for templating in a second catanionic system (CTAT/SDBS), although the silica particles appear to be less stable in this case. The sizes of the hollow silica particles obtained are consistent with the sizes of equilibrium vesicle used for templating, ranging from about 60 to 120 nm. Hollow silica particles of desired size can thus be gained by tuning the size of the surfactant vesicles by changing the surfactant ratio or concentration.

Table 1. Composition of Silica Samples Prepared from CTAB/FC₇ Vesicles

sample	δ	γ (wt%)	$m(\text{CTAB/FC}_7)/$ $m(\text{TMOS})$	silica morphology
SVT1	0.8	1.9	0.5	hollow spheres
SVT2	0.8	1.9	1	hollow spheres
SVT3	0.8	1.9	2	gelation
SVT4	0.85	2	1	hollow spheres
SVT5	0.85	3	1	hollow spheres
SVT6	0.85	3.5	1	hollow spheres
SVT7	0.44	2	1	multilamellar structures

Templating within the biphasic region of the CTAB/FC₇ phase diagram resulted in more complex morphologies. Reactions carried out during equilibration of the lamellar/vesicular phase reveal initially the presence of hollow silica nanospheres, followed at later times by the formation of much larger and multilamellar structures that are perhaps intermediate states encountered during the formation of the lamellar mesophase.

Acknowledgment. We acknowledge the support of the National Institute of Standards and Technology, Gaithersburg, MD, an agency of the Technology Administration, U.S. Department of Commerce, in providing facilities used in this work. H.P.H. is grateful for the financial support of the German Academic Exchange Service (DAAD) and CAM is grateful for the financial support of the National Science Foundation Grant CTS-9814399.

LA020727W